J Appl Electrochem (2008) 38:1771–1778
DOI 10.1007/s10800-008-9628-x

ORIGINAL PAPER

Influence of constant magnetic field on the electrodeposition of Co–Mo–W alloys

M. Zieliński · E. Miękoś

Received: 27 December 2007 / Accepted: 30 June 2008 / Published online: 29 August 2008
© Springer Science+Business Media B.V. 2008

Abstract The aim of this study was to investigate the effect of a constant magnetic field (CMF) on the electrodeposition of Co–Mo–W alloys, and to observe changes in the topography of the alloy surface and its chemical composition. The investigation included the use of Cyclic Voltammetry (CV), Coulometry (C), Scanning Electron Microscopy (SEM) and Energy Dispersive X-ray Analysis (EDX). At higher electrolyte concentrations (so-called II), the CV method revealed an increase in cathode current density in a CMF environment. During crystallisation of the Co–Mo–W alloy, fractures appeared on the surface due to internal stresses. The application of CMF reduced the fracture widths resulting from the increased concentration of electroactive particles at the working electrode and the greater deposited alloy mass. Electrolyte motion under the influence of CMF caused an increase in the percentage of the main ferromagnetic component (Co) in the alloy.

Keywords Alloys · Constant magnetic field (CMF) · Electrodeposition · Magnetohydrodynamics (MHD) · Lorentz force

1 Introduction

One of the major problems facing applied electrochemistry involves the process of making electrodes with specific surface chemical and phase compositions. However, this can be done by depositing layers of transition metal alloys. Studies on alloys have focussed on what are known as functional metallic layers characterised by specific physicochemical properties, including mechanical, electrical, magnetic and optical. To improve the properties of binary and ternary alloys (with cobalt as the main component), other metals are introduced which are characterised by better physical properties than those possessed by cobalt alone. For example, the physical properties required are found in molybdenum and tungsten. Some of the physical properties of these metals are shown in Table 1.

Molybdenum and tungsten cannot be deposited from aqueous solutions; however, they can be co-deposited inductively [1] with Fe, Co and Ni metals. This phenomenon has not been fully explained; the current opinion is that the co-deposition of tungsten and molybdenum with iron-group metals takes place as a result of the reduction in heteropolytungstates or heteropolymolybdates [2, 3]. Much effort has been put into explaining the mechanism of this phenomenon and its application in industry. Ni and Fe are the most frequently used metals due to the fact that they are cheaper than others. Molybdenum and tungsten, apart from having good physical properties, are transition metals showing catalytic properties in electrode processes, and they easily form interstitial compounds. It has been demonstrated that metals with more unpaired electrons in the *d*-orbital interact more strongly with electrodonating atoms or molecules.

The content of Mo in these alloys is proportional to the concentration of Mo in the electrolyte, while the W content is considerably lower. The composition of the alloys depends on several factors, such as electroplating solution composition, electrolysis conditions, base metal type and cathode shape. A fracture network appears on the surface of Co–Mo–W alloys during the crystallisation process, a phenomenon related to the existence of high internal stresses in the alloys. The magnitude of the internal stresses

M. Zieliński (✉) · E. Miękoś
Department of General and Inorganic Chemistry, University of Lodz, Narutowicza 68, 90-136 Lodz, Poland
e-mail: zielmark@chemul.uni.lodz.pl

Table 1 Physical properties of the metals forming ternary Co–Mo–W alloys

Physical properties	Cobalt (Co)	Molybdenum (Mo)	Tungsten (W)
Melting point (°C)	1495	2610	3410
Conductivity (S m^{-1})	17.2×10^6	18.7×10^6	18.9×10^6
Hardness (HB)	125	255	400
Strength (MPa)	680	2500	1500

depends on the quantity of the individual metals in the electrolyte and the layer thickness of the deposited alloy. Internal stresses are created when the tensile stresses in the metallic coating are higher than the strength of the alloy coating. In such a case, the alloy tends to increase in volume. An additional parameter which changes the character of the electrodeposition reaction is the constant magnetic field (CMF) environment. The previous assumption was based on the fact that the majority of transition metals demonstrate paramagnetism, caused by the presence of unpaired electrons. Both Mo and W are paramagnetic, whereas the main component (Co) is ferromagnetic.

As far as the application of a CMF is concerned, various results have been published on the influence of a magnetic field on the electrodeposition of metals and alloys [4–6]. A 30% increase in the cathode current was observed during the electrodeposition of Cu in an external magnetic field with an induction of 0.7 T [7]. Matsushima et al. [8] reported that grains of Fe electrodeposited without the influence of a magnetic field had sharp ends, and their sizes were larger than grains electrodeposited in a magnetic field, the latter being rounded. Msellak et al. [9] proved that Ni-Fe alloys deposited in a magnetic field with an induction of 0.9 T were smoother, had a uniform structure and featured a preferential grain orientation. It was also shown that the magnetic field causes a magnetohydrodynamic effect (MHD) during the convection process when a Lorentz force is applied [10].

Daniluk et al. [11] analysed CV curves obtained during the electrodeposition of Cu in a magnetic field of $B =$ 0–0.178 T. They ascribed the phenomenon to the MHD effect, which intensifies the convection process (as well as the motion of ions and molecules) in the electrolyte, leading to an increase in both the Faradaic and limiting current. O'Reilly et al. [12] found that under the influence of a CMF, an increase in the current density (*j*) occurred, caused by the decreasing thickness of the diffusion layer (δ_D): $j = (n \cdot F \cdot D \cdot C)/\delta_D$, where: *j*—limiting current density, *n*—number of electrons participating in the reaction, *F*—Faraday constant, *D*—diffusion coefficient, *C*—concentration of electroactive ions in the body of the electrolyte, δ_D—diffusion layer. Leventis and Gao [13] presented the theory of mass flow in an electrolyte consisting of paramagnetic molecules. Lioubashevski et al. [14] developed a theoretical hydrodynamic model demonstrating the influence of a magnetic field on electrochemical processes. Moreover, they defined an empirical formula for calculating the value of current depending on the magnetic induction applied: $i \approx C^{3/4} \cdot B^{1/3}$. They showed how the thickness of the diffusion layer near the electrode decreases under the influence of a magnetic field. Bund et al. [15, 16] demonstrated the role of magnetic forces in electrochemical reactions during the anodic solubilization of copper in a magnetic field of $B = 0.6$ T. They showed six different spatial orientations of the magnetic field direction with regard to the working electrode surface as well as the direction of the formation of the magnetic force in relation to a positively charged, paramagnetic molecule. Ragsdale and White [17, 18] showed microscopic images confirming magnetohydrodynamic flow in the electrolyte, demonstrating that the flow is more intense when the direction of vector (**B**) is parallel to the working electrode surface than when it is perpendicular to the working electrode surface. They examined the reduction in nitrobenzene on a platinum disk electrode with induction $B = 0$; 0.1; 0.3 and 0.5 T. Leventis et al. [19] examined the dependence of the direction of magnetic force (F) on the angle between magnetic field vector (**B**) and the direction of current (i) at disk electrodes.

2 Experimental

Cyclic Voltammetry (CV), Coulometry (C), Scanning Electron Microscopy (SEM) and Energy Dispersive X-ray Analysis (EDX) were used. A three-electrode system was used consisting of the following components: a working (gold, disk) electrode of 0.1 cm^2 surface area, an auxiliary platinum mesh electrode of much larger area and a saturated calomel reference electrode. The working electrode was prepared mechanically (with the use of sandpaper P2000 grit), chemically (using a chromic acid cleaning mixture) and electrochemically (polarisation in a stock solution of 0.01 M H_2SO_4, within the potential range of -1.5 V to $+1.5$ V, with a sweep rate of 100 mV s^{-1}). The measuring system was located between the pole shoes of an N–S pole electromagnet (Fig. 1).

The magnetic induction (**B**) applied during measurements ranged from 0 to 1.2 T, and the magnetic induction vector was parallel to the surface of the working (gold, disk) electrode. The less concentrated (concentration I) electrolyte used in the electroplating bath consisted of the following components: 0.1 M of $CoSO_4$; 0.01 M of

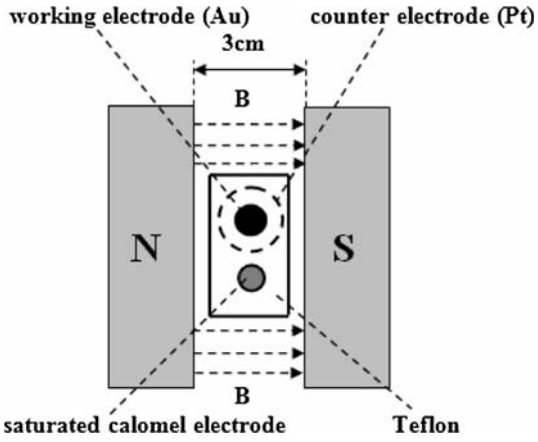

Fig. 1 Scheme of the measuring system

Na_2MoO_4; 0.01 M of Na_2WO_4; 0.2 M of sodium citrate and 0.01 M of H_2SO_4. The more concentrated electrolyte (concentration II) consisted of the following components: 0.27 M of $CoSO_4$; 0.07 M of Na_2MoO_4; 0.06 M of Na_2WO_4; 0.45 M of sodium gluconate; 0.1 M of citric acid; 0.025 M of EDTA and 0.01 M of H_2SO_4. A Co–Mo–W alloy was deposited at a potential of -1.17 V_{SHE} (-1.42 V_{SCE}) over a period of 3500 second. The criterion of optimization of alloy deposition potential was based on the CV curve (Fig. 2).

On the basis of initial tests, the deposition potential of the Co–Mo–W alloy was determined as being optimal for this electrode and these particular experimental conditions. CV and the coulometry tests were carried out with the use of the following components: a laboratory electromagnet with N and S pole shoes (ER-2505 type), a electrochemical cell with a three-electrode system, a PZP-80 control device for the electromagnet, a stable current source for the electromagnet, a Hall sensor for a constant magnetic field, a Hall teslameter (TH-26 type), and equipment for the electrochemical tests: ATLAS 99 (9933 Electrochemical Interface, and 9923 Frequency Response Analyser) and computer (with the following software: POL-99 and IMP-99). SEM measurements were performed with the use of a scanning electron microscope (Vega 5135 MM from Tescan), commonly used for testing the surface morphology of Co–Mo–W alloys. For the EDX tests, an X-ray microanalyser (EDX Link 300 ISIS from Oxford Instruments) was used for both the qualitative and quantitative analysis of the chemical composition of the Co–Mo–W alloy.

3 Results and discussion

The purpose of this paper was to investigate changes caused by the application of CMF during the electrodeposition processes of Co–Mo–W alloys, as well as to observe changes concerning the morphology and chemical composition of the resulting ternary alloys. During the tests carried out in a CMF, magnetohydrodynamic forces *(F)* appeared in the electrolyte, according to the Lorentz formula [12, 14, 15, 20, 21]:

$$F = j \times \mathrm{B} \tag{1}$$

where: j—limiting current density vector; B—magnetic induction vector.

Figure 3 shows the vectors of the forces that influenced the charge of the flowing ions and induced the electrolyte to move along the surface of the working (gold) electrode. The force vectors were observed from two different directions (1 and 2), the angle between which being 90°. In

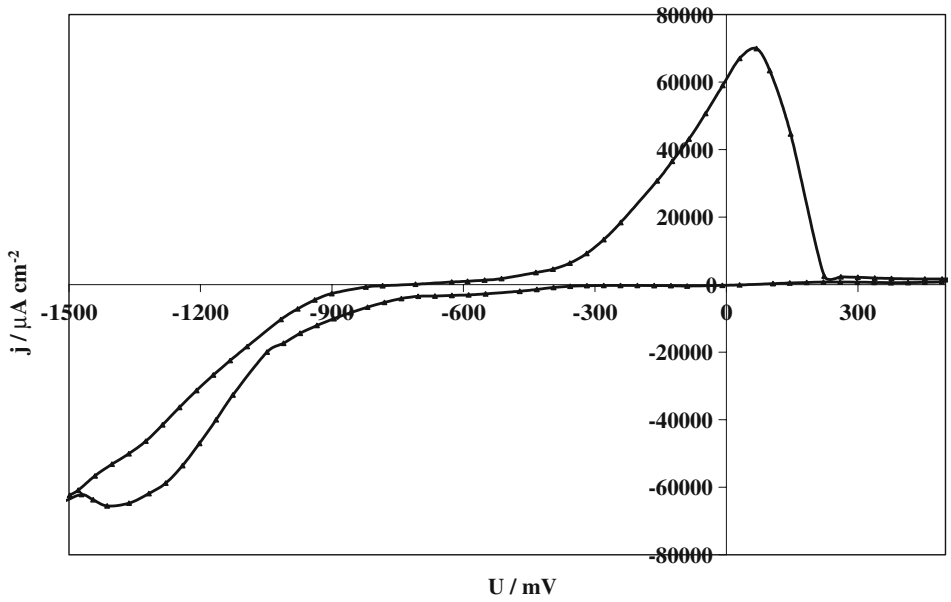

Fig. 2 The cyclic chronovoltammogram for Co–Mo–W alloy (concentration II)

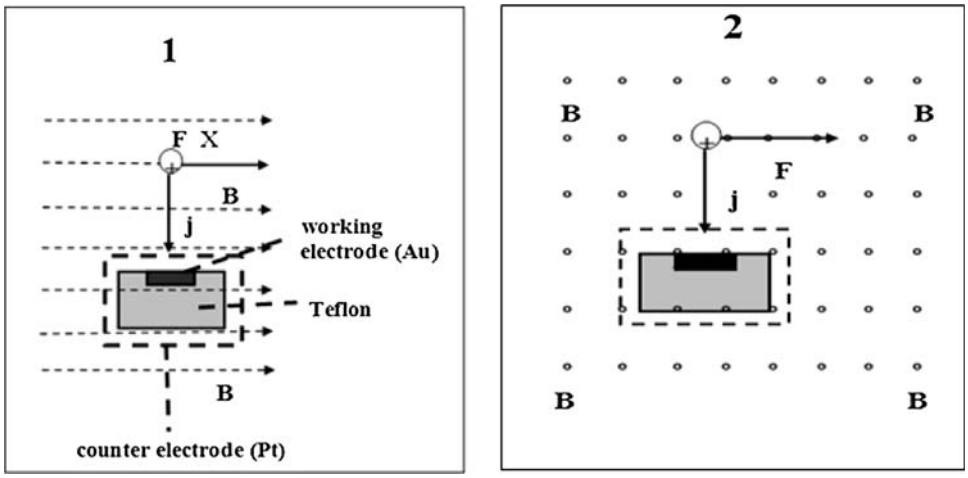

Fig. 3 Direction of the magnetohydrodynamic force (F) created as a result of the effect of a CMF on a positively charged paramagnetic molecule when observed from two directions (1 and 2), the angle between which is 90°

the case of direction 1, the force vector (**F**) is contained in the area shown in the figure, with the magnetic induction vector (**B**) pointing to the right. For direction 2, the magnetic induction vector (**B**) comes out of the plane, while the force vector (**F**) points to the right.

Electrolyte concentration I was developed on the basis of earlier investigations by other authors [22], but the effects of the concentration were not related to the CMF. For concentration I, the effects of the magnetic field were found to be marginal. Due to the too low concentration of electroactive ions in the electrolyte, the catalytically active sites on the working electrode were occupied by the other components from the electrolyte solution, especially as a result of the electrolyte motion, caused by the magnetohydrodynamic forces. The electrolyte with a higher concentration (II) was used as a result of theoretical considerations. With the use of the CV method, it was shown that the effect of magnetic induction (B) on cathodic currents was significant in this case. The densities of the cathodic currents of the ternary Co–Mo–W alloys were compared with those of the cathodic currents of the binary Co–Mo alloys, with regard to both concentrations, i.e. I and II (Fig. 4). The cathodic current density was measured at potential -1.17 V_{SHE} (-1.42 V_{SCE}).

Consequently, the effect of the CMF, in this case expressed as an increase in the cathodic current density, depends on the concentration of electroactive particles. This was particularly evident in the case of the Co–Mo–W alloy for electrolyte concentration II. This phenomenon is in accordance with the theoretical model of Fahidy and Aogaki [14, 23, 24]:

$$j = (4.3 \cdot 10^3) n^{3/2} A^{-1/4} D v^{-1/4} C^{4/3} B^{1/3} \quad (2)$$

as well as with the quantitative model of Lioubashevski [14]:

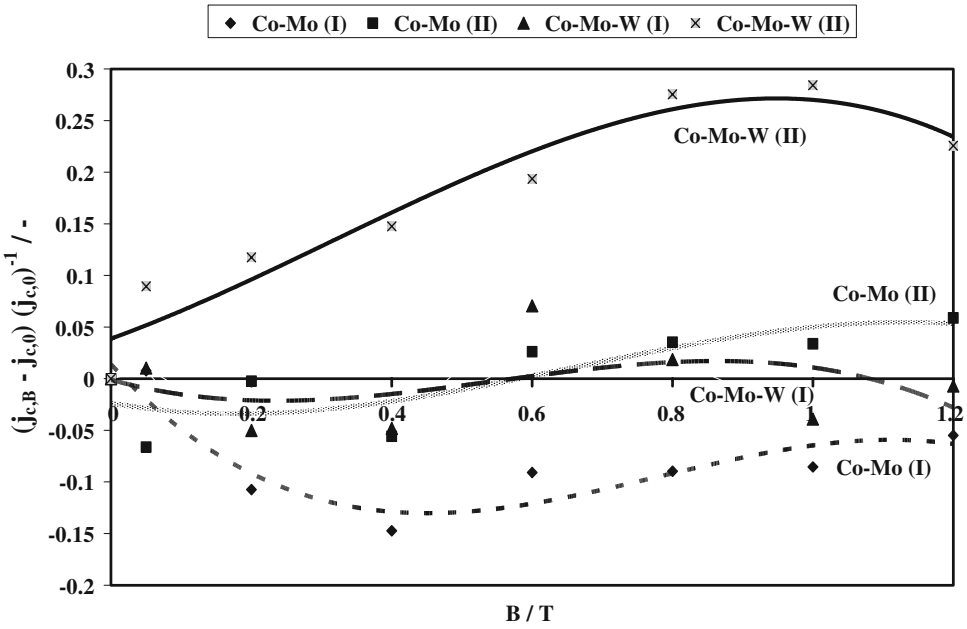

Fig. 4 Comparison of cathodic current densities [as expressed by the relationship $(j_{c,B}-j_{c,0})(j_{c,0})^{-1}$] as a function of magnetic induction (B) in the process of electrodeposition of Co–Mo and Co–Mo–W alloys, where: $j_{c,B}$—cathodic current density in a CMF, $j_{c,0}$—cathodic current density ($B = 0$), (concentration I): 0.1 M of $CoSO_4$; 0.01 M of Na_2MoO_4; 0.01 M of Na_2WO_4; 0.2 M of sodium citrate and 0.01 M of H_2SO_4, (concentration II): 0.27 M of $CoSO_4$; 0.07 M of Na_2MoO_4; 0.06 M of Na_2WO_4; 0.45 M of sodium gluconate; 0.1 M of citric acid; 0.025 M of EDTA and 0.01 M of H_2SO_4

$$j \approx 0.63\pi^{1/6}A^{-1/6}\rho^{-1/3}D^{8/9}v^{-2/9}(nFC)^{4/3}B^{1/3} \quad (3)$$

where: j—limiting current density; n—number of electrons participating in the reaction; A—working electrode area; D—diffusion coefficient; N—kinematic viscosity of the electrolyte; C—concentration of electroactive ions in the body of the electrolyte; B—magnetic induction P—density of electrolyte F—Faraday's constant.

On the basis of the Coulometry (C) measurements, the relationship between the charge (Q) flowing in the electrolyte and magnetic induction (B) were determined for Co, specific Co–Mo and Co–Mo–W alloys for electrolyte concentrations I and II. Figure 5 indicates that the more complicated the structure of the metallic coating, i.e. Co, Co–Mo, Co–Mo–W, the higher the value of magnetic induction (B) required to achieve maximum effect of the CMF on the charge (Q).

Scanning Electron Microscopy (SEM) was used to study the surface of Co–Mo–W alloys obtained with and without a magnetic field for electrolyte concentrations I and II. The topography of the working electrode surface always plays a highly significant role in an electrochemical reaction. The heat and free enthalpy of adsorption vary over the surface and, consequently, the catalytically active locations, characterised by the highest free enthalpy of adsorption, are filled first and only then are the remaining sites filled. As mentioned earlier, fractures are formed during the crystallisation of Co–Mo–W alloys due to the internal stresses existing in these alloys. When the electrolyte with higher concentration (II) was used, fractures occurred less frequently on the surface, but the fracture widths were larger. This phenomenon is visible in Fig. 6, for $B = 0$, at 1000× magnification. This was obviously due to the greater mass of the deposited alloy and consequently to the greater alloy thickness.

Further analysis of the surface topography of Co–Mo–W alloys shows that the use of CMF reduced the width of the fractures formed due to internal stresses. This phenomenon was visible at both 1000× and 5000× magnification (see Fig. 7 for concentration II).

The phenomenon occurred because the thickness of the Nernst diffusion layer (δ_D) at the working electrode surface was reduced under the influence of the CMF:

$$\delta_D \approx 1.59(\rho R v^{2/3}D^{1/3})^{1/3}(nFCB)^{-1/3} \quad (4)$$

where: R—radius of the working disk electrode. Consequently, the concentration of electroactive ions (C_{el}) at the electrode increased and a larger amount of the alloy was deposited:

$$m \approx 0.63(\rho R)^{-1/3}v^{-2/9}D^{8/9}(nFCB)^{1/3} \quad (5)$$

where:——mass of alloy

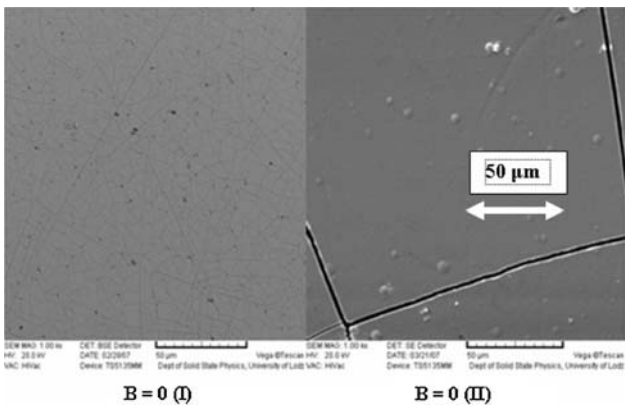

Fig. 6 Comparison of Co–Mo–W alloy surfaces at concentrations I and II

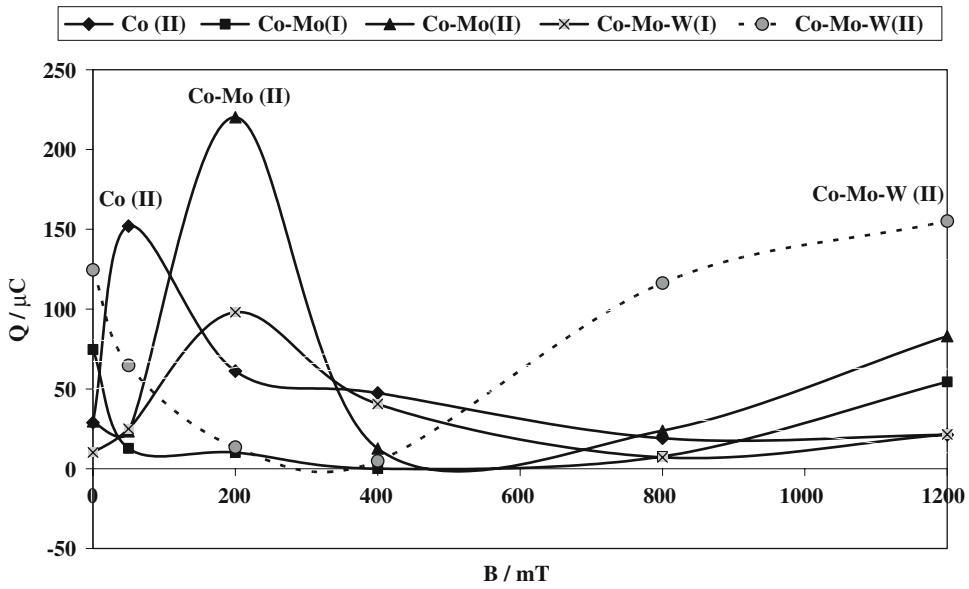

Fig. 5 The relationship between the charge (Q) and magnetic induction (B) during the electrodeposition reaction of Co and Co–Mo and Co–Mo–W alloys

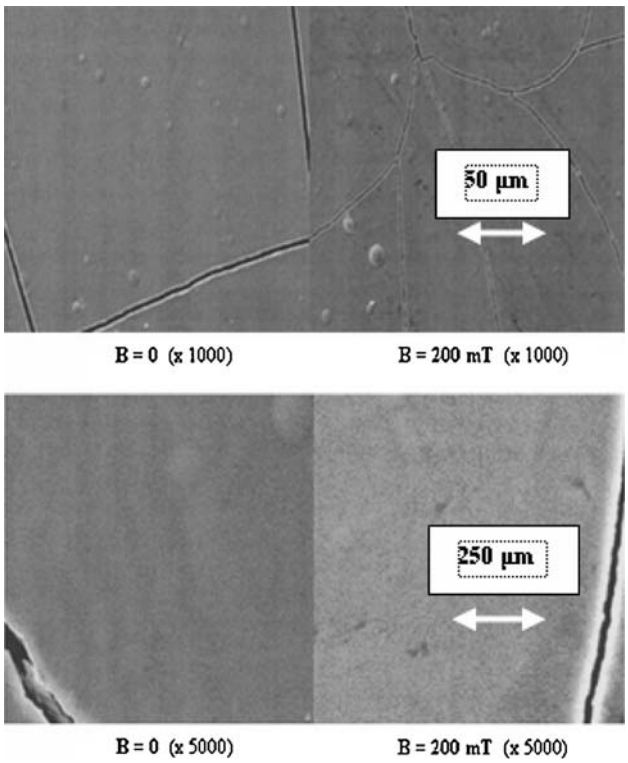

Fig. 7 Reduction in fracture widths on the surface of Co–Mo–W alloy obtained at concentration II under the influence of a CMF

With an increased amount of deposited alloy, the fracture widths occurring as a result of internal stresses were reduced. In accordance with theoretical considerations, the Lorentz magnetic forces under the experimental conditions resulted in the motion of the electrolyte being tangential to the working electrode surface and perpendicular to the magnetic induction vector, **B**. A laminar and unidirectional (x-direction) flow of electrolyte was assumed. A Navier-Stokes hydrodynamic layer (δ_H) was formed, resulting in a reduction in the diffusion layer (δ_D). Figure 8 shows the probable manner in which these layers were formed during the experiment.

The vector of magnetic induction (**B**) in Fig. 8 comes out of the figure plane. C is the concentration of electroactive particles inside the electrolyte, while C_{el} is the concentration at the electrode; ($\boldsymbol{j}$) is the current density vector (in the y-direction) and U is the velocity vector of electroactive particles (in the x-direction). The value of U can be calculated from the Navier-Stokes equation [25, 26]:

$$\rho[\partial U/\partial t + (U + \nabla)U] = -\nabla P + \eta \Delta U + F_i \qquad (6)$$

where: ∇—Del operator $(\nabla = \partial/\partial x + \partial/\partial y + \partial/\partial z)$; Δ—Laplace differential operator $(\Delta = \nabla^2 = \partial^2/\partial x^2 + \partial^2/\partial y^2 + \partial^2/\partial z^2)$; η—dynamic viscosity of the electrolyte

The terms on the left side of the equation show the increase in the parameter values characterising the liquid. On the right side of the equation:$(-\nabla P)$ describes the pressure gradient; $(\eta \Delta U)$ describes the friction force, and F_i describes the external forces exerted on the liquid. From the Bernoulli equation, which shows that during the steady liquid flow the sum of the kinetic energy, potential energy, pressure and position for the mass unit of a flowing liquid are constant, it follows that the pressure of the external regions of a liquid is constant. Consequently, the term $(-\nabla P)$ can be omitted. The external force (F_i) influencing the liquid is the Lorentz magnetic force (F). Therefore, the following equation can be formulated for the x-direction of the liquid motion:

$$\rho U_x(\partial U_x/\partial x) = \eta(\partial^2 U_x/\partial y^2) + F \qquad (7)$$

The term $[\eta(\partial^2 U_x/\partial y^2)]$ can be rewritten as $[\eta(U/\delta_H^2)]$ because the y-direction specifies the thickness of the Navier-Stokes hydrodynamic layer. The magnetic force F must overcome the friction force $[\eta(U/\delta_H^2)]$. Since the force $(nFCBD/\delta_D)$ has already been calculated, the following approximate formula can be defined:

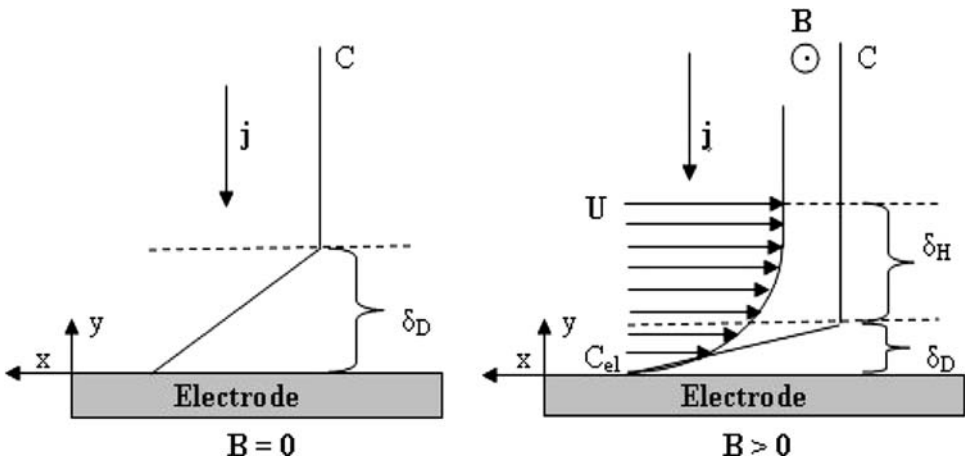

Fig. 8 Reduction in the Nernst diffusion layer thickness (δ_D) near the working electrode surface under the influence of a CMF, and formation of the Navier-Stokes hydrodynamic layer (δ_H), where: C—concentration of electroactive ions in the body of the electrolyte, C_{el}—concentration near the working electrode, x, y—direction

Table 2 Composition of electrolyte concentrations I and II and composition of Co–Mo–W alloys obtained from these electrolytes both with and without a CMF, examined using Energy Dispersive X-ray Analysis (EDX)

Metallic elements	% Mass in electrolyte	% Mass in Co–Mo–W alloy, $B = 0$	% Mass in Co–Mo–W alloy, $B = 200$ mT
Concentration I			
Co	67.8	55.4	52.1
Mo	11.0	42.0	44.9
W	21.2	2.6	3.0
Concentration II			
Co	42.3	84.7	87.9
Mo	20.0	11.9	9.1
W	32.8	3.5	3.0

$$\eta(U/\delta_H^2) \approx (nFCBD)/\delta_D \tag{8}$$

Also, it was found that $\delta_D \approx 0.62\,\mathrm{Pr}^{-1/3}\,\delta_H$, where $\mathrm{Pr} = D/\nu = (D \cdot \rho)/\eta$ (Prandtl number). Consequently, the following can be formulated:

$$\begin{aligned} U &\approx (nFCDB\,\mathrm{Pr}^{1/3}\,\eta^{-1}\delta_H)/0.62 \\ &\approx (nFCD^{4/3}B\rho^{1/3}\delta_H)/(0.62\eta^{4/3}) \end{aligned} \tag{9}$$

Based on Eq. 9 one can state that the velocity of the electroactive particles *(U)* increases with the increase in magnetic induction (*B*). The increase in *B* is also accompanied by an increase in the thickness of the Navier-Stokes hydrodynamic layer *(δ_H)* which determines electrolyte flow under the influence of a CMF. The chemical composition of the Co–Mo–W alloys was examined using Energy Dispersive X-ray Analysis (EDX). Parameters of the research were as follows: the energy of electrons (10 keV), the system resolution (63 eV) and the special resolution (0.5 μm). Table 2 lists the mass percentages of the individual metals present in the electrolyte, as well as in the Co–Mo–W alloy, both obtained with ($B = 200$ mT) and without a CMF.

As shown in Table 2, the percentages of the individual metallic components (Co, Mo, W) of the electrolyte do not correspond to similar contents in the Co–Mo–W alloy, which is in agreement with earlier research. The percentage increase in Mo and W concentrations in electrolyte II did not produce good results because these elements can only be deposited with other metals, in this case with Co, whereas the percentage concentration of this element in electrolyte II was lower. In the case of low concentration of electroactive ions in electrolyte I, the effect of the electrolyte motion in the CMF was that the active sites of the working (gold) electrode were occupied by diamagnetic molecules of the stock solution, which resulted in a decreased content of the main component (Co) at $B = 200$ mT (% values of Mo and W filled the remaining spaces). For the higher concentration (II) of electroactive ions of the main component (Co), the motion of the electrolyte in the CMF meant that a larger number of ions of the ferromagnetic material (Co) occupied the active sites on the gold electrode and took part in the electrodeposition, causing a percentage increase in the amount of ferromagnetic material in the resulting Co–Mo–W alloy.

4 Conclusions

The use of a higher concentration of electrolyte (II) showed an increase in the cathodic current density during the process of depositing the Co–Mo–W alloy, caused by an increase in the magnetic induction value (B). The coulometry method (C) demonstrated that the more complicated the structure of metallic coating, the higher the value of magnetic induction (B) required for the CMF to achieve maximum influence on the charge value (Q). The (SEM) revealed that the application of a CMF resulted in a decrease in the width of the surface fractures, which had been formed as a result of internal stresses in the Co–Mo–W alloy during crystallization. On the basis of the EDX method, it was found that CMF contributed to an increase in the percentage content of the ferromagnetic component (Co) in the Co–Mo–W alloy, provided that its concentration in the electrolyte before the electrodeposition was sufficiently high.

Acknowledgment The work was supported by Lodz University Grant No 505/717

References

1. Brenner A (1963) Electrodeposition of Alloys. Academic Press, New York, London
2. Vas'ko AT, Kowach SK (1983) Elektrokhimiya tugoplavkih metallov. Tekhnika, Kiev
3. Griffiths DJ (1998) Introduction to electrodynamics, Prentice Hall
4. Ciba A, Ogawa T, Yamashita T (1988) Surf Coat Technol 34:455
5. Nikolic ND, Wang H, Cheng H, Guerrero CA, Garcia N (2004) J Magn Magn Mater 2436:272–276
6. Li XP, Zhao ZJ, Seet HL, Heng WM, Oh TB, Lee JY (2004) Electrochem Solid State Lett 7(1):C1
7. Mohanta S, Fahidy TZ (1972) Can J Chem Eng 50:248

8. Matsushima H, Nohira T, Mogi I, Ito Y (2004) Surf Coat Technol 179:245
9. Msellak K, Chopart JP, Ibara O, Aaboubi O, Amblard J (2004) J Magn Magn Mater 281:295
10. Tacken RA, Janssen LJJ (1995) J Appl Electrochem 25:1
11. Daniyuk AL, Kurmashev VI, Matyushkov AL (1990) Thin Solid Films 189:247
12. O'Reilly C, Hinds G, Coey IMD (2001) J Electrochem Soc 148(10):C674
13. Leventis N, Gao X (2001) Anal Chem 73:3981
14. Lioubashevski O, Katz E, Willner J (2004) J Phys Chem B 108:5778
15. Bund A, Kohler S, Kuhnlein HH, Plieth W (2003) Electrochim Acta 49:147
16. Bund A, Kuehnlein HH (2005) J Phys Chem B 109:19845
17. Ragsdale SR, Grant KM, White HS (1998) J Am Chem Soc 120:13461
18. Ragsdale SR, White HS (1999) Anal Chem 71:1923
19. Leventis N, Chen M, Gao X, Canalas M, Zhang P (1998) J Phys Chem B 102:3512
20. Tabakovic I, Riemer S, Vas'ko V, Sapozhnikov V, Kief M (2003) J Electrochem Soc 150(9):C635–C640
21. Tabakovic I, Riemer S, Sun M, Vas'ko V, Kief M (2005) J Electrochem Soc 152(12):C851–C860
22. Gomez E, Pellicer E, Alcobe X, Valles E (2004) J Solid State Electrochem 8:7
23. Fahidy TZ (1973) Electrochim Acta 18:607
24. Aogaki R, Fueki K, Mukaibo T (1975) Denki Kagaku 43:504
25. Perry JH (1974) Chemical Engineers' handbook. McGraw-Hill, New York
26. Sissom LE, Pitts DR (1972) Elements of transport phenomene. Mc Graw-Hill, New York